Robust Control of Homogeneous Azeotropic Distillation Columns

Elling W. Jacobsen, Lionel Laroche, and Manfred Morari
Chemical Engineering, California Institute of Technology, Pasadena, CA 91125

Sigurd Skogestad
Dept. of Chemical Engineering, University of Trondheim, N-7034 Trondheim, Norway

Henrik W. Andersen
Dept. of Chemical Engineering, Technical University of Denmark, DK-2800 Lyngby, Denmark

The entrainer feed used in homogeneous azeotropic distillation provides an extra degree of freedom in the steady-state design compared to simple distillation. In this article, we discuss the control of azeotropic distillation columns in the region close to minimum entrainer feed. Both industrial experience and previous research indicate that this is a difficult task. However, by considering the high-frequency behavior (initial response) of the column, we show that tight and robust control can be obtained with simple single-loop PI controllers. The results depend on the presence of high-frequency phenomena such as flow dynamics.

Introduction

Binary mixtures forming minimum boiling azeotropes are commonly encountered in the chemical industry. The separation of such mixtures into the pure components is not possible by simple distillation and must be accomplished by other means. In homogeneous azeotropic distillation, the separation is made feasible by adding a third component called the entrainer. The entrainer alters the thermodynamic properties of the mixture, thereby enabling separation of the binary azeotrope into the pure components. This type of distillation is widespread in the process industry, and the economic potential of improved operation is usually high.

Distillation is the unit operation that has received most attention in the process control community. However, almost all the work so far has been concentrated on ideal binary distillation. The main reason for this is probably that even simple distillation columns are hard to understand and control. In homogeneous azeotropic distillation, several complexities are added: nonideal thermodynamics, multicomponent mixtures, and multiple feeds. Most articles in this area have concentrated on modeling the thermodynamics, selection of entrainers (for example, Doherty and Caldarola, 1985; Laroche and Morari, 1992), steady-state design (for example, Levy and Doherty, 1985a, b), and optimizing the separation (for example, Knight and Doherty, 1989). Only a few articles have been devoted to the control problem: Abu-Eishah and Luyben (1985), Andersen et al. (1989), Anderson (1989), Bozenhardt (1988), and Gilles et al. (1980). Most of them have studied specific cases, and few general conclusions are drawn. Andersen et al. (1989) presented a more general analysis, but mainly based on steady-state arguments. The most significant conclusion to draw from the articles is that homogeneous azeotropic distillation columns seem to be much more difficult to control than simple distillation columns. This appears to be supported also by industrial experience.

The entrainer used in homogeneous azeotropic distillation columns provides an extra degree of freedom compared to simple distillation. As several authors have shown (Andersen et al., 1989), this degree of freedom may be used to optimize the operation in terms of entrainer and utility (heating and cooling) consumption. However, steady-state arguments indicate a much more difficult control problem at the steady-state optimal operating point than at operating points with higher utility consumption (Andersen et al., 1989). This has led some authors to concentrate also on nonoptimal operating points (Knapp and Doherty, 1990). Industrial experience also shows that it is a common practice to operate far from the

E. W. Jacobsen is presently at the Dept. of Chemical Engineering, University of Trondheim, NTH, N-7034 Trondheim, Norway.
L. Laroche is presently with Procter & Gamble, Canada.
Correspondence concerning this article should be addressed to M. Morari.

ticles for these bubbles show a particle-to-particle *cohesion* which dominates the particle-to-bubble *adhesion*, resulting in the formation of large clusters which are unable to adhere to a hydrogen bubble in water.

Acknowledgment

The authors wish to thank Mrs. M. Mittelmeyer-Hazeleger of the University of Amsterdam for determining the physical properties of the catalyst particles and Mr. G. Bierman for performing part of the experiments.

Notation

A = BET-specific surface area of catalyst particles, $m^2 \cdot kg^{-1}$
Eo = modified Eötvös number $= (\rho_P - \rho_L) g R_P^2 / \sigma_{LG})$, 1
F = force, N
F_A = apparent weight of a particle in a liquid, N
F_{AC} = apparent weight of a cluster consisting of n_C equal-sized spherical particles in a liquid, N
$F_{i,j}$ = component of the apparent weight of a particle positioned under an angle $i \cdot \Delta\alpha$ (Figure 4), N
F_i^* = contribution of all the particles positioned on parallel i of a globe with radius $R_B + R_P$ to the downward force exerted on the lowest particle, N
F^* = total downward force exerted on the lowest particle by all other particles of the adhering monolayer, N
F_C = capillary force, N
F_P = force due to the capillary pressure in the gas bubble, N
g = acceleration due to gravity ($g = 9.81$ m·s^{-2}), m·s^{-2}
n = maximum number of parallels with adhering particles, 1
$(n_A)_{max}$ = maximum number, defined in Eq. 25, 1
n_C = number of equally sized particles in a cluster (Figure 2), 1
$(n_C)_{max}$ = maximum value of n_C, 1
N_A = total number of adhering particles at the gas-bubble surface, 1
N_i = number of adhering particles positioned on parallel i of the globe with radius $R_B + R_P$, 1
N_{tot} = total number of adhering particles in a monolayer covering the bubble completely, 1
$P_{i,j}$ = intersection point of parallel i and meridian j of the globe with radius $R_B + R_P$, 1
P_σ = capillary pressure in a gas bubble, N·m^{-2}
r = radius of the three-phase contact ring (Figure 2), m
R_B = radius of a gas bubble, m
R_P = radius of a catalyst particle, m
V_P = specific pore volume of a particle, $m^3 \cdot kg^{-1}$

Greek letters

$\Delta\alpha$ = angle between centers of two neighboring particles adhering to a gas bubble (Figure 4), rad
$i \cdot \Delta\alpha$ = angle indicating the position of a particle at a gas bubble surface (Figure 4), rad
α_{max} = measured maximum angle of bubble-surface coverage, rad
ζ = fraction of the gas-bubble surface area covered by catalyst particles (Eq. 32), 1
θ = G/L/S contact angle, rad
θ^* = minimum value of θ required for complete bubble-surface coverage, rad
θ_E = effective G/L/S contact angle, rad
θ_0 = contact angle at zero curvature of the contact line, rad
κ = line energy, N
λ = ratio of particle and bubble radii ($\lambda = R_P/R_B$), 1
ρ_G = density of the gas phase, kg·m^{-3}
ρ_L = density of the liquid phase, kg·m^{-3}
ρ_P = density of the particle with pores filled with liquid, kg·m^{-3}
ρ_{SK} = density of the solid part of a dry catalyst particle, kg·m^{-3}
σ_{LG} = static surface tension of a gas-liquid interface, Pa·m
σ_{SG} = surface tension of solid-gas interface, Pa·m
σ_{SL} = surface tension of solid-liquid interface, Pa·m
φ = angle characterizing the immersion depth of a particle, rad
φ_m = minimum value of φ_s before the particle is released from the gas bubble where $n_C = (n_C)_{max}$, rad
φ_s = angle characterizing the immersion depth of a particle under static conditions, rad
ψ = physical quantity defined in Eq. 33, 1

Literature Cited

Ayala, R. E., E. Z. Casassa, and G. D. Parfitt, "A Study of the Applicability of the Capillar Rise of Aqueous Solutions in the Measurement of Contact Angles in Powder Systems," *Powder Technol.*, **51**, 3 (1987).

Heertjes, P. M., and N. W. F. Kossen, "Measuring the Contact Angles of Powder-Liquid Systems," *Powder Technol.*, **1**, 33 (1967).

Kossen, N. W. F., and P. M. Heertjes, "The Determination of the Contact Angle for Systems with a Powder," *Chem. Eng. Sci.*, **20**, 593 (1965).

Langmuir, I., "Oil Lenses on Water and the Nature of Monomolecular Expanded Films," *J. Chem. Phys.*, **1**, 756 (1933).

Lindner, D., and M. Werner, and A. Schumpe, "Hydrogen Transfer in Slurries of Carbon Supported Catalyst (HPO Process)," *AIChE J.*, **34**, 1691 (1988).

Neumann, A. W., and R. J. Good, "Techniques of Measuring Contact Angles," *Surf. Colloid. Sci.*, **11**, 31 (1979).

Scheludko, A., B. V. Toshev, and D. T. Bojadjiev, "Attachment of Particles to a Liquid Surface (Capillary Theory of Flotation)," *J. Chem. Soc. Trans. Farad.*, **72**, 2815 (1976).

Schulze, H. J., "Physico-Chemical Elementary Processes in Flotation," *Developments in Mineral Processing*, **4**, Elsevier Science, New York (1984).

Sell, P. J., A. W. Neumann, "Die Oberflächenspannung fester Körper," *Angew. Chem.*, **6**, 321 (1966).

Sell, P. J., "Randwinkelmessungen an pulverförmigen Stoffen," *Phys. Chem. Anwendungstech.*, **3**, 23 (1972).

Wimmers, O. J., "The Enhancement of Gas-Absorption by a Heterogeneously Catalysed Chemical Reaction," PhD Thesis, Univ. of Amsterdam (1987).

Wimmers, O. J., and J. M. H. Fortuin, "The Use of Adhesion of Catalyst Particles to Gas Bubbles to Achieve Enhancement of Gas Absorption in Slurry Reactors: I. Investigation of Particle-to-Bubble Adhesion Using the Bubble Pick-Up Method," *Chem. Eng. Sci.*, **43**, 303 (1988).

Manuscript received Jan. 14, 1991, and revision received Aug. 28, 1991.

Table 1. Data for Acetone-Heptane-Toluene Column

F	z_F	E	z_{E1}	z_{E2}	N	NF	NE	y_D	r_{12}
1.0	0.90	*)	1.e−7	1.e−4	33	6	27	0.998	0.005

Reboiler is tray No. 1.
Feed and entrainer are saturated liquids.
Total condenser with saturated reflux.
Liquid holdups are M_i/F = 0.5 min including reboiler and condenser (no additional accumulators).
Constant molar flows.
Equilibrium calculated by Van Laar activity coefficient model.

*)	Operating Point	II_B	II_A	V_{min}	I_A	I_B
	E_6	0.46	0.50	0.57	1.00	2.00

steady-state economic optimum, perhaps due to a belief of easier operation with increased entrainer consumption. Knight and Doherty (1989), in their study on an industrial column, found that it used seven times more entrainer than what would be optimal.

In this article, we will concentrate on the high-frequency (initial-response) dynamics of the system. It is the initial response of the open-loop system that determines the feedback control properties. The frequency region around the expected closed-loop bandwidth (approximately 0.01 − 1 min^{-1}) is most important. In our analysis, we will use the frequency-dependent relative gain array (RGA) (Bristol, 1966, 1978) and the closed-loop disturbance gain (Hovd and Skogestad, 1991). The frequency-dependent relative gain array has proven to be an efficient tool for evaluating controllability of simple distillation columns, and the closed-loop disturbance gain seems to have promising properties when evaluating the effect of disturbances under feedback control.

We start the article by presenting briefly the separation sequence in homogeneous azeotropic distillation and then the model used in the analysis. This model includes important high-frequency characteristics usually excluded in control studies of distillation columns. The analysis of the model presented subsequently deals with both different operating points and different control configurations. The selection of an appropriate control configuration has proven to be essential for the control of simple distillation columns. The ultimate test of controllability is obviously the design of controllers with an optimized performance. We use the structured singular value (Morari and Zafiriou, 1989) as a criterion. In this manner, we

Table 2. Data for Ethanol-Water-Ethylene Glycol Column

F	z_F	E	z_{E1}	z_{E2}	N	NF	NE	y_D	r_{12}
1.0	0.87	*)	1.e−7	1.e−4	50	17	48	0.998	0.0001

Reboiler is tray No. 1.
Feed and entrainer are saturated liquids.
Total condenser with saturated reflux.
Liquid holdups are M_i/F = 0.5 min including reboiler and condenser.
Constant molar flows.
Equilibrium calculated by Van Laar activity coefficient model.

*)	Operating Point	II_B	II_A	V_{min}	I_A
	E	0.35	0.75	1.00	2.00

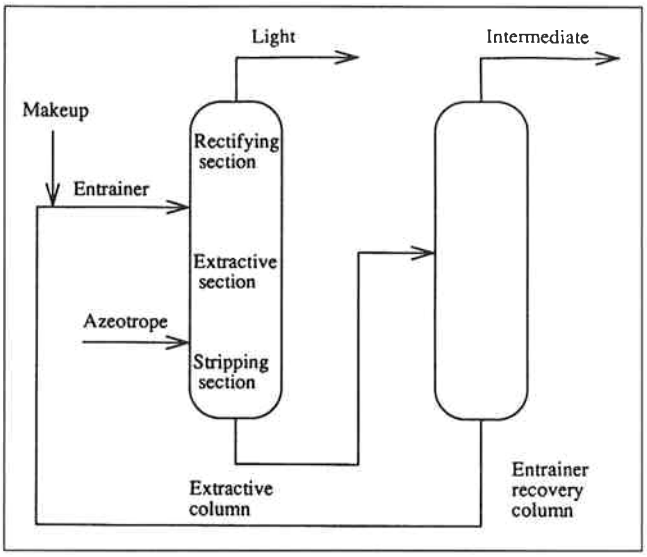

Figure 1. Separation sequence for the case of minimum boiling binary azeotrope and heavy entrainer.

may study the effect of model uncertainty that is of utmost importance when designing controllers for ill-conditioned plants (Skogestad et al., 1988). We conclude the article by discussing how optimal operation may be obtained in practice.

We will use an example column that separates a mixture of acetone, heptane, and toluene (AHT). Acetone and heptane form a minimum boiling azeotrope, and toluene is used as an entrainer. Toluene is the least volatile component in the mixture. Data for the column are given in Table 1. Control design results will also be presented for a column separating a system of ethanol, water, and ethylene glycol. Data for this column are given in Table 2.

Separation Sequence

In homogeneous azeotropic distillation, an entrainer is added to make the separation feasible. Therefore, the system consists of three components, and two columns are needed to separate the mixture. The sequence in which this separation takes place will be determined by the type of entrainer used. The entrainer used most commonly in the industry is a heavy boiler, which is the least volatile component of the mixture. We only consider this type of system here. In the case of a heavy entrainer we recover in the first column, called the extractive column, the lightest component at the top and a mixture of the intermediate and the heavy component at the bottom. The bottom product is fed to the second column, the entrainer recovery column, for separation of the binary mixture. The entrainer product from the recovery column is fed back to the extractive column. In the case of heavy entrainer, the entrainer will be fed into the upper part of the column. The separation sequence is shown in Figure 1.

Because of the two feeds to the extractive column, we have three sections in the column compared to two in the ideal binary case (see Figure 1). The main purpose of the extractive section is to separate the components of the binary azeotrope. In the rectifying section the entrainer is removed from the top product, while in the stripping section light component is removed

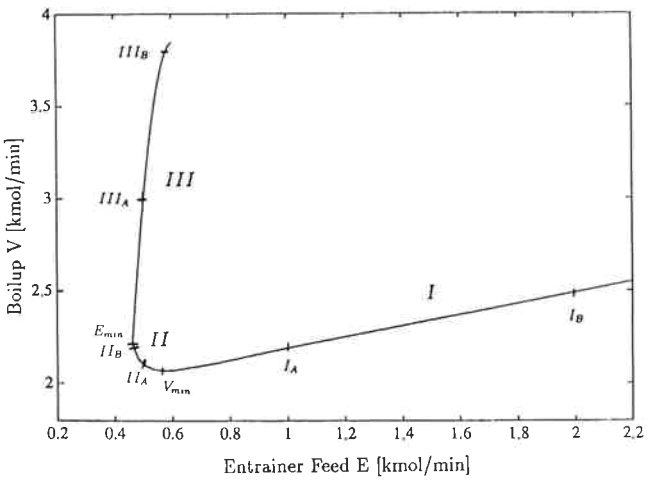

Figure 2. Set of operating points for the acetone-heptane-toluene column.

from the bottom product. For a more detailed discussion on the significance of different sections, we refer to the work by Andersen et al. (1989).

As pointed out by Andersen et al., one must be careful when making specifications in the bottom product of the extractive column as this will determine the achievable separation in the recovery column. More specifically, all the light component in the bottom product of the extractive column will enter the top product of the recovery column as impurity. To make sure that the fraction of impurity does not exceed a desired value we must limit the fraction of light to intermediate component in the bottom product of the first column. As specifications for the extractive column, we will therefore use:

y_D = fraction of light component in the distillate

r_{12} = ratio of light to intermediate component in the bottom product

The specifications for the AHT column are: $y_D = 0.998$ and $r_{12} = 0.005$.

Steady-state optimal operation

As stated above, the entrainer feed may be used to optimize the column for a given separation. Andersen et al. (1989) showed that by varying the entrainer feed flow and adjusting the other flows accordingly for a given separation, one obtains a continuous set of possible operating points. They described the set in the form of an entrainer feed/boilup relation. For the AHT column studied in this article we obtain the set of operating points shown in Figure 2. The set of operating points may be divided into three distinct regions.

Region I. A decrease in entrainer feed leads to a decrease in boilup and thereby to a more optimal operation with decreased entrainer consumption.

Region II. At a certain point the boilup reaches a minimum (V_{min}), and a further decrease in entrainer feed results in increased boilup. This will continue until we reach the minimum entrainer needed for the separation (E_{min}). The optimal operating point will be between E_{min} and V_{min}. The exact location of the optimal operating point will depend on the cost of entrainer and heating/cooling.

Region III. The third region is caused by an input multiplicity in the system and was discovered by Andersen et al. In this region an increased entrainer feed gives a sharp increase in boilup.

Andersen et al. have discussed in detail the origin of the different regions.

The rest of the article is devoted to analyzing the controllability in the different regions. The operating points we will consider are named I_A, I_B, V_{min}, II_A, II_B, III_A, and III_B, as shown in Figure 2. We will assume operating point II_A to be optimal and will hence concentrate on this operating point. Operating point II_B is located almost at E_{min}.

We will not discuss the control of the recovery column as it basically may be considered as an ideal binary column. The coupling of the two columns is discussed briefly toward the end of the article.

Modeling

The full nonlinear dynamic model used has three states per tray. The states are expressed as the fraction of two components plus liquid holdup on each tray. For the AHT column this implies a total of 102 states. The flow dynamics are described by a linear relation between liquid flow and liquid holdup:

$$L_i = L_i^o + (M_i - M_i^o)/\tau_L \tag{1}$$

where superscript o denotes nominal steady-state values. τ_L is computed from a linearized Francis weir formula:

$$\tau_L = \frac{2}{3}\frac{M_{oi}}{L_i} \tag{2}$$

where M_{oi} denotes liquid over weir and L_i is the liquid flow. We use a holdup on each tray equal to $M_i/F = 0.5$ min and assume half of the liquid over the weir. The flow dynamics usually are not included in models for control studies of distillation columns, but have an important high-frequency effect. As shown by Skogestad et al. (1990a), the flow dynamics introduce a lag in reflux from the top to the bottom of the column that leads to a decoupling at high frequencies.

The equilibrium is modeled by the Van Laar activity coefficient model. We assume constant molar flows, that is, we exclude the energy balance.

In the analysis and controller design we make use of linearized models. Due to the high order of the full models we use reduced models with 20 states. The models were reduced by means of a balanced minimal realization.

In simple distillation we have been successful using simplified models with only one or two time constants (Skogestad and Morari, 1988). We found it difficult to obtain good and general models in this way for the extractive column. Hence, we will not use such models here.

Shinskey (1977) proposed using logarithmic composition measurements as a simple means of reducing the effect of nonlinearities. We will adopt this for the extractive column and will hence use the following measurements in the rest of the article:

$$\log(1 - y_D) \tag{3}$$

$$\log(r_{12}) \tag{4}$$

The logarithm does also give a good scaling of the outputs:

$$\Delta y_D^s = \frac{\Delta y_D}{1 - y_D} \tag{5}$$

$$\Delta r_{12}^s = \frac{\Delta r_{12}}{r_{12}} \tag{6}$$

where the superscript s denotes scaled variables.

Control Configurations

In control terms a distillation column may be viewed as a 5×5 system: five manipulated variables (L, V, D, B, and V_T) and five primary outputs (y_D, r_{12}, M_D, M_B, and P). The feed streams are assumed to be given here (disturbances). One could design a full multivariable controller where all manipulated variables are coupled to all the measurements. This would, of course, be optimal from a theoretical point of view. For practical reasons, however, it is common to design a decentralized controller with five single loops. Such a controller is easier to understand and to retune and will also be more failure-tolerant. We will assume such a decentralized controller structure in this work.

When using a decentralized control structure, the first decision usually made is selection of level loops. The selection of which inputs to be used for level control is often considered part of the column design. The decision made here, however, is of vital importance for the remaining control problem. Different control configurations will have different dynamic characteristics. This has been pointed out by several authors for the case of simple distillation (Shinskey, 1984; Skogestad et al., 1990a). We will consider here four different configurations: LV, DV, DB and (L/D)(V/B) configurations. The names indicate which inputs are left for composition control; for example, the LV configuration refers to using reflux L and boilup V to control compositions. The DB configuration would be rejected from steady-state arguments ($D + B = F$), but as shown by Skogestad et al. (1990b), it may be a good choice for simple distillation columns due to its high-frequency characteristics. It also shows how misleading steady-state arguments can be when evaluating processes for controllability. Skogestad et al. (1990a) found the (L/D)(V/B) configuration to be the best overall selection for a series of simple distillation columns they studied.

Open-Loop Dynamics

Region III.

Andersen et al. (1991) found that the operating points in the undesirable region III had severe right-half-plane zeros. They found that these right-half-plane zeros were due to a negative effect of internal flows ($dL = dV$) on separation in this region. The *rhp* zeros are related to the input multiplicity found in the set of operating points (see Figure 2). For the AHT column we find the worst *rhp* zero at 0.234 at operating point III_A and at 0.128 at operating point III_B. Because these *rhp* zeros impose serious bandwidth limitations and because the operating points in region III are clearly nonoptimal, it is unlikely that the column would be operated in this region. We will, therefore, exclude these operating points from any further analysis.

Region I and II

To get an idea of how the dynamics of the extractive column vary with operating conditions we will consider the open-loop gains of the LV configuration at the different operating points. That is, we consider the gains in the transfer matrix:

$$\begin{bmatrix} d\log(1 - y_D) \\ d\log(r_{12}) \end{bmatrix} = G^{LV} \begin{bmatrix} dL \\ dV \end{bmatrix} \tag{7}$$

Figure 3 shows the open-loop gains as a function of frequency for the LV configuration at the different operating points. Note that the outputs are scaled according to Eqs. 5 and 6.

For responses of the bottom composition we see that there are only small differences between the different operating points. The responses are essentially first order, as in most simple distillation columns, with a dominant time constant around 500 min. From the figure we also see that the response from reflux to bottom composition breaks off at higher frequencies. This is caused by the lag introduced by the flow dynamics.

For responses in the top composition we see that there are significant differences between the different operating points. Furthermore, the responses are dominated by higher-order dynamics than those in the bottom. There is an initial effect with a time constant around 4 min and a slower effect with a time constant similar to what is observed for responses in the bottom composition. The two poles are separated by a zero, and the system is minimum phase.

In general there are two separate effects in distillation: 1. the initial effect due to changes in flows (not to be confused with flow dynamics) and 2. a slow effect due to interaction between adjacent tray compositions (Rademaker et al., 1975). Skogestad and Morari (1988) showed that for most simple distillation columns the slope of the initial response will usually be prolonged by the slow secondary response, thereby resulting in an overall first-order response. This is mainly a result of the interaction between *all* the compositions in the column and will not be true for all columns.

In columns with pinches in the composition profiles (almost no difference in composition between two trays), the interaction between the top and bottom of the column will vanish, and we may get higher-order responses. Extractive columns will usually have pinches for one or several components, and we may, therefore, experience higher-order dynamics. In the AHT column for instance, we have a pinch for acetone in the top of the extractive section.

Weigand et al. (1972) have also shown that in many cases the responses in the top and bottom of simple distillation columns may differ significantly. They found that the dominating time constant in general will apply only to the end with the largest absolute change in composition. This corresponds well to what we find here where the absolute change is largest in the bottom.

Comparing the different operating points we see that the main differences in the top composition responses are at low frequencies, while the high-frequency dynamics (initial re-

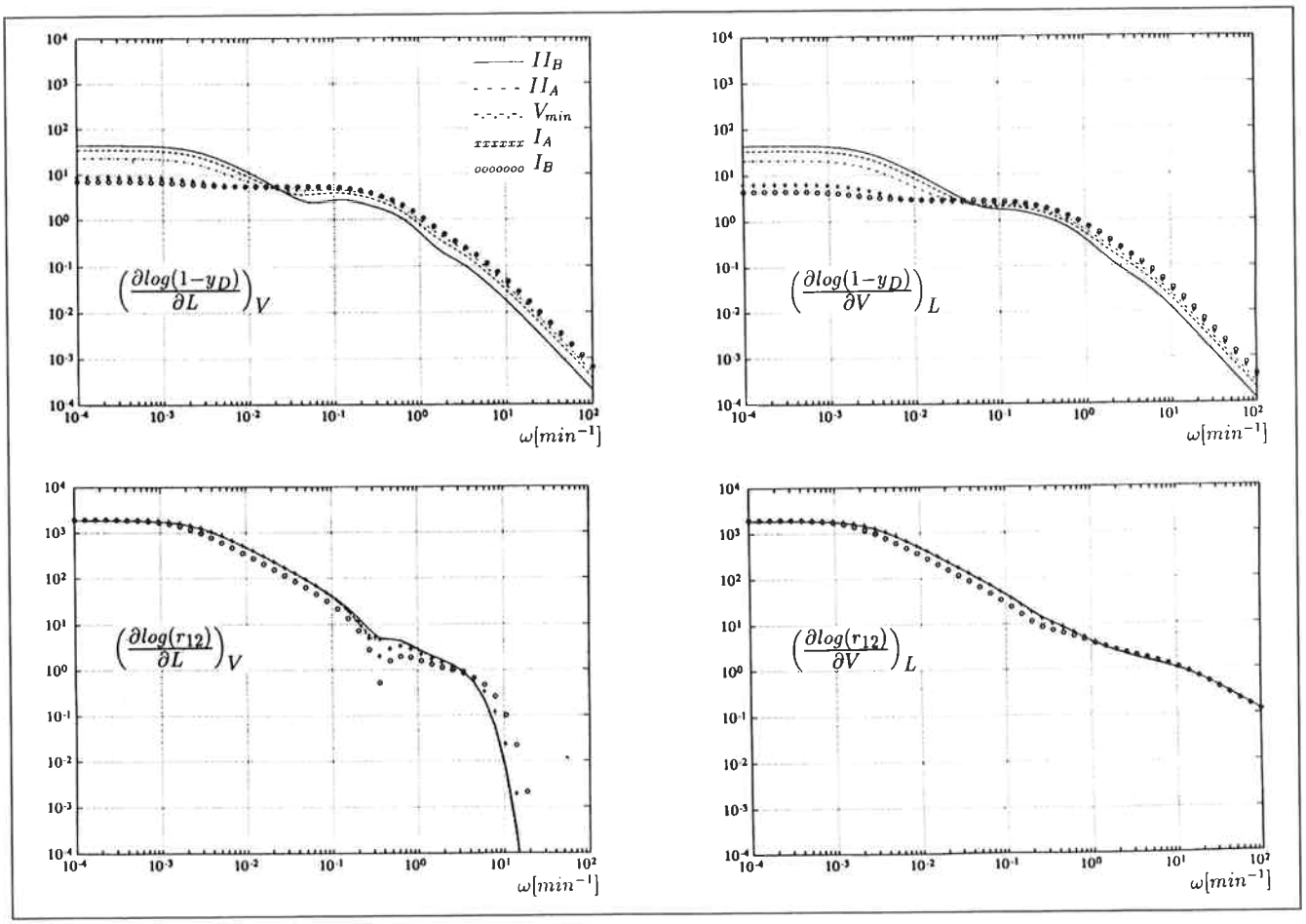

Figure 3. Open-loop gains for the *LV* configuration at different operating points.

sponses) are similar at all the operating points. The large difference in steady-state gains between different operating points may be explained by the fact that different sections of the column will dominate at different operating points (Andersen et al., 1989). Skogestad and Morari (1988) found also for simple distillation that the initial responses are less dependent on the operating conditions than the low-frequency responses.

We conclude that while the low-frequency dynamics may differ widely between operating points, there are only small differences at high frequencies for responses both in the top and bottom compositions. For control purposes the high-frequency dynamics are most important, and based on the open-loop dynamics we would, therefore, not expect big differences between the control properties observed at the different operating points.

For the other configurations we find similar results: that is, small differences between the high-frequency dynamics at the different operating points. The only exception is the (L/D) (V/B) configuration. The gains for this configuration in terms of single flow gains may be expressed in the form:

$$d(L/D) = \left(\frac{1}{D}\right)dL - \left(\frac{L}{D^2}\right)dD \tag{8}$$

and

$$d(V/B) = \left(\frac{1}{B}\right)dV - \left(\frac{V}{B^2}\right)dB \tag{9}$$

Between the different operating points we have only small variations in distillate $D(D \approx Fz_F)$, while the bottoms product B will vary significantly since almost all the entrainer leaves in this product. Reflux L and boilup V will also vary somewhat (see Figure 2). The variations in flows imply that while the gains for the single flows vary only slightly, the gains for the ratios will vary significantly with the operating point. This may, however, be compensated for by measuring the flows, which is necessary anyway with this configuration.

Relative Gain Array

The relative gain array (RGA) was proposed originally by Bristol (1966) as a steady-state interaction measure and has found widespread application for selecting single-loop pairings in decentralized control. One of the main advantages of the RGA is that it depends only on the model itself and, therefore, does not require any preliminary controller design. This is due to the assumption of "perfect control." Another advantage of the RGA is that it is scaling-independent.

The RGA may easily be extended to a frequency dependent measure (Witcher and McAvoy, 1977; Bristol, 1978) and will in this case contain more useful information with respect to

feedback control. We are interested primarily in the frequency region around the expected closed-loop bandwidth. The definition of the elements in the RGA is given by:

$$\lambda_{ij}=\frac{(\partial y_i/\partial u_j)_{u_{l\neq i}}}{(\partial y_i/\partial u_j)_{y_{l\neq i}}}=g_{ij}(s)[G^{-1}(s)]_{ji} \tag{10}$$

As the elements in each row and column sum up to unity in the RGA (Bristol, 1966), we only have to consider the (1, 1) element for the 2 × 2 case. The (1, 1) element for the 2 × 2 case is given by:

$$\lambda_{11}=\frac{1}{1-\dfrac{g_{12}(s)g_{21}(s)}{g_{11}(s)g_{22}(s)}} \tag{11}$$

where g_{ij} denotes the (i, j) element of the transfer matrix G.

Skogestad et al. (1990a) successfully used the frequency-dependent RGA for selecting control configurations in simple distillation, and Hovd and Skogestad (1990) have proven its usefulness on a more general basis. Besides giving information on interaction among single loops, the RGA also contains useful information on sensitivity to input uncertainty. Another measure that is frequently used to assess controllability is the condition number, γ. However, the condition number is scaling-dependent, and the minimized condition number γ^* is used instead. Skogestad and Morari (1987a) give the following relationship between the RGA and the minimized condition number for 2 × 2 plants:

$$\|\Lambda\|_1-\frac{1}{\gamma^*}\leq\gamma^*\leq\|\Lambda\|_1 \tag{12}$$

where $\|\Lambda\|_1$ denotes the 1-norm of the RGA. Thus, the difference between $\|\Lambda\|_1$ and γ^* is at most equal to $1/\gamma^*$. Since $\|\Lambda\|_1$ is much easier to compute, it is the preferred quantity to use.

Figure 4 shows the RGA as a function of frequency for the four configurations at the different operating points. From the figure we see that for all the configurations the RGA differs widely between the operating points at steady state. For the LV configuration we have, for instance, a steady-state value of 70 at operating point II_B and a steady-state value of less than 3 in I_B. From the steady-state RGA one would, therefore, have concluded that the control problem is much more difficult in the optimal region II than in the nonoptimal region I. The same conclusion would be reached for the (L/D)(V/B) configuration, while interestingly enough one would reach the

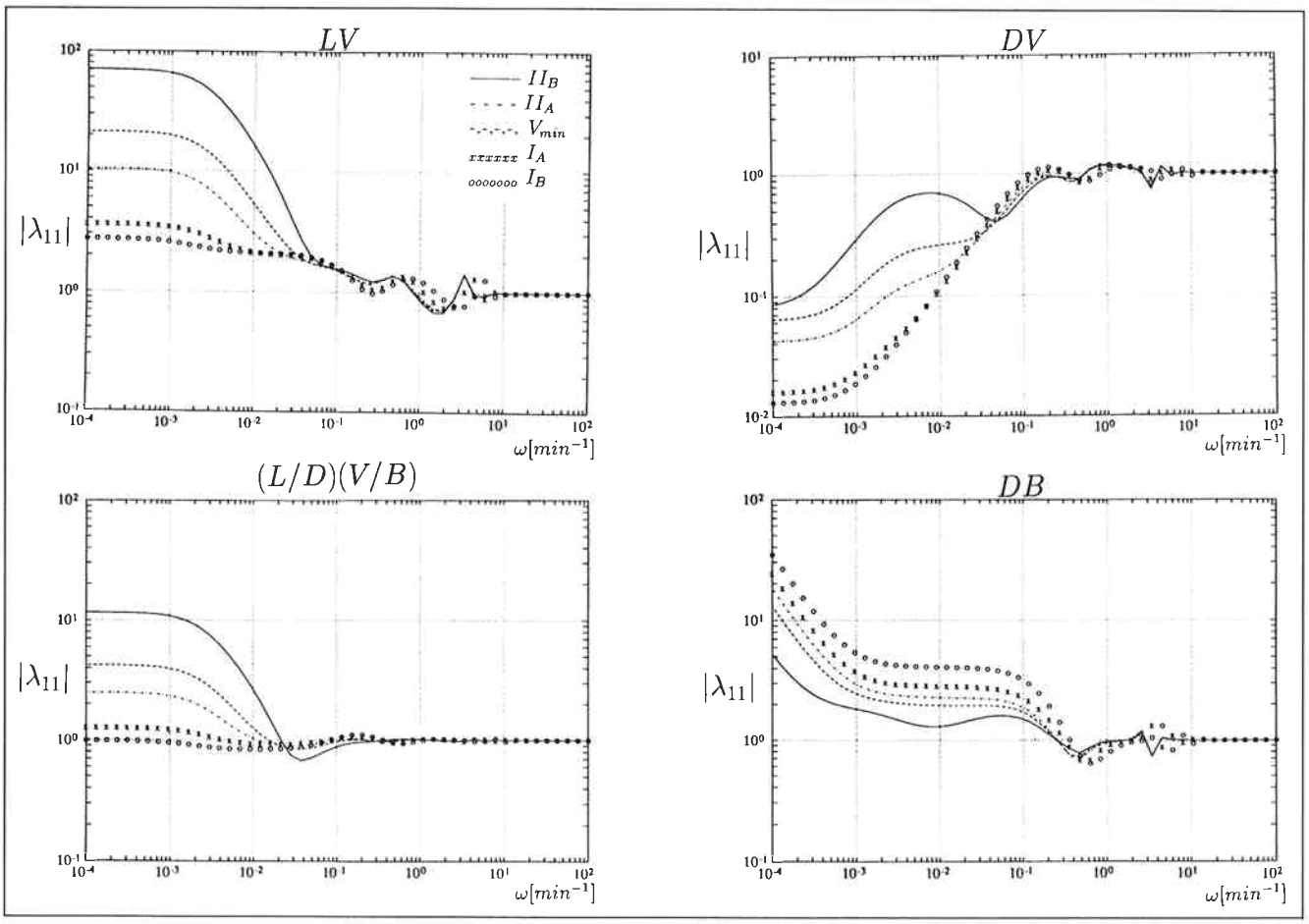

Figure 4. RGA as a function of frequency for the configurations LV, DV, DB and (L/D)(V/B) at different operating points.

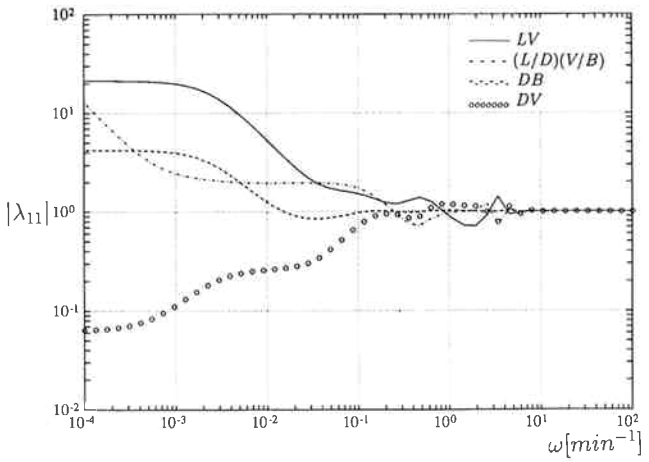

Figure 5. RGA as a function of frequency for the configurations LV, DV, (L/D)(V/B) at operating point II_A.

opposite conclusion for the DV and DB configuration. However, we stress that steady-state arguments may be misleading in the analysis for control. It is more important that the RGA's at higher frequencies are similar at all the operating points. This is not surprising because we have seen that the high frequency dynamics are similar at the different operating points. At high frequencies all the RGA values reach a value of one due to the decoupling introduced by the flow dynamics.

The steady-state RGA values for the DV configuration are less than 0.5 at all the operating points, which would suggest to pair the distillate D with the bottom composition r_{12} and the boilup V with the top composition y_D. This is counterintuitive on physical grounds. We also note that this suggestion is valid only for low frequencies. At higher frequencies the RGA is above 0.5 and, therefore, the usual pairing is suggested, e.g., pairing D with y_D and V with r_{12}. Similar RGA plots are also obtained for simple distillation columns with higher purity in the top than in the bottom (Skogestad et al., 1990).

To compare the configurations we have plotted the RGA values of the four configurations at the optimal operating point II_A in Figure 5. The plot shows that the (L/D)(V/B) has a RGA value equal to one from a frequency of approximately 0.01 min^{-1} and upwards, and seems to be a favorable configuration. The RGA plot also indicates that the control problem at operating point II_A is relatively simple when we use the (L/D)(V/B) configuration.

We conclude from the RGA analysis that with a properly-tuned controller (reasonably high bandwidth) and a "good" configuration we would not expect any worse control problems in the optimal region II than in region I. The RGA values are

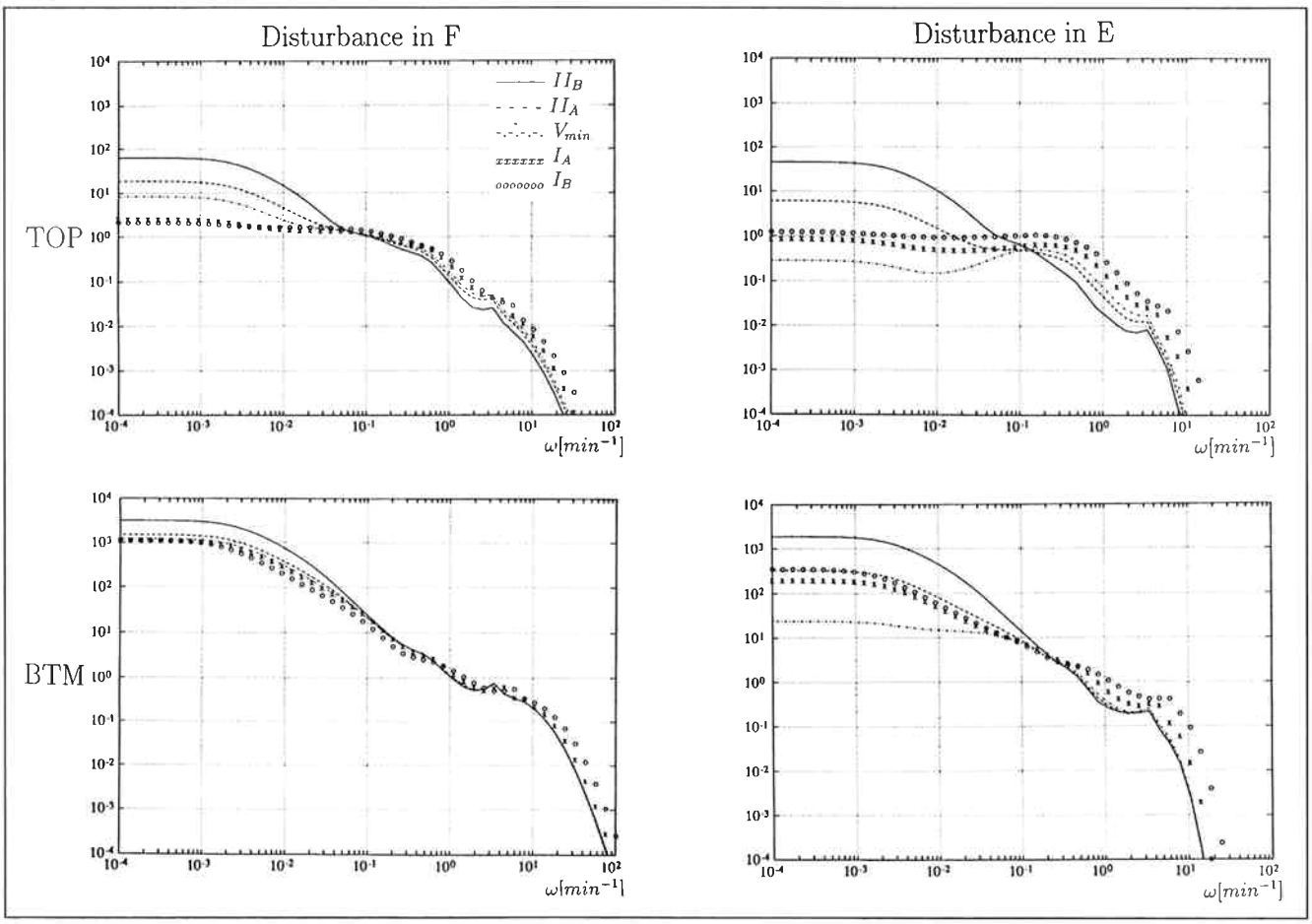

Figure 6. Closed-loop disturbance gains for disturbances in *F* and *E* using configuration LV at different operating points.

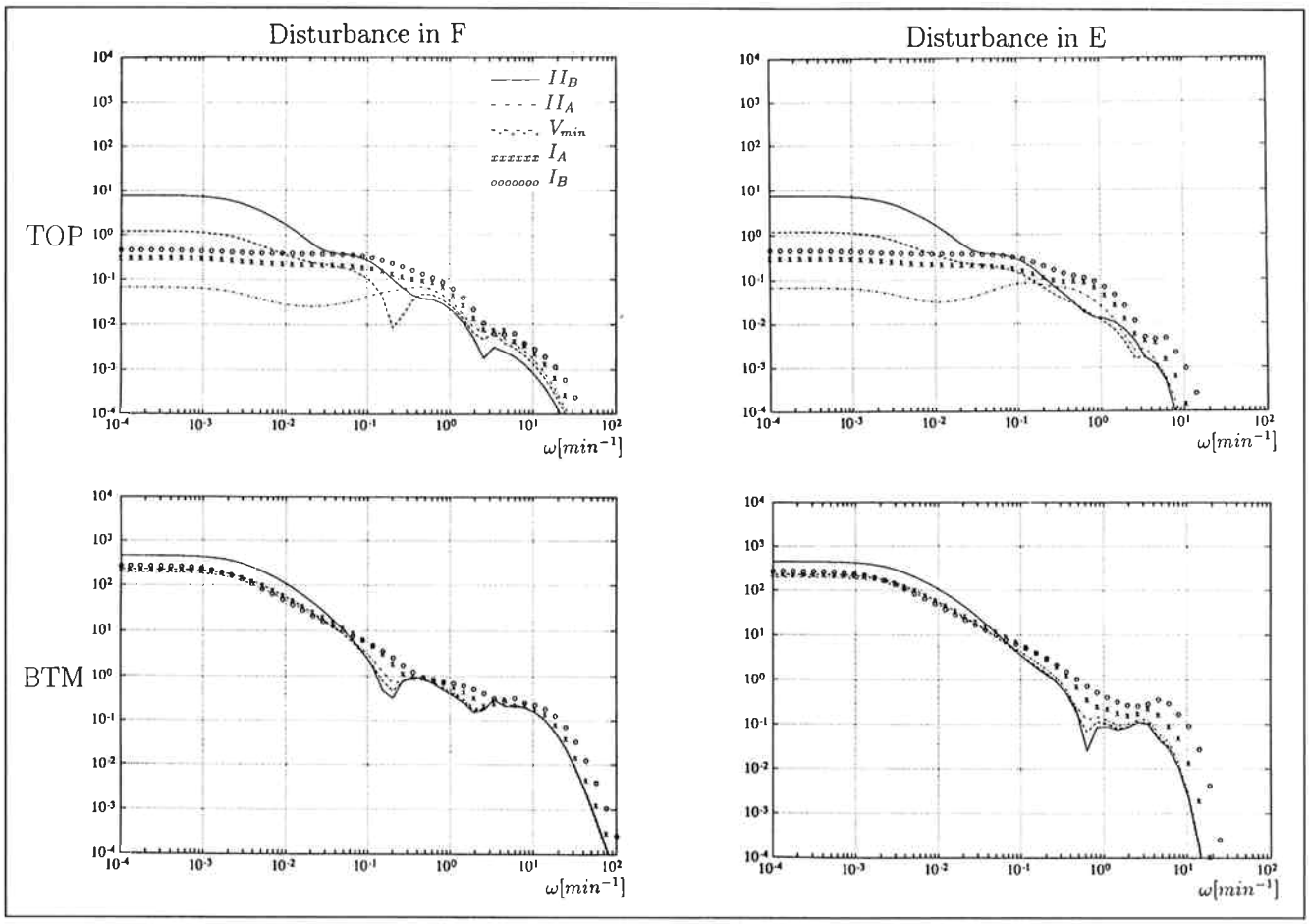

Figure 7. Closed-loop disturbance gains for disturbances in *F* and *E* using configuration (L/D)(V/B) at different operating points.

also comparable to what has been found in simple distillation and do, therefore, not indicate a more difficult control problem for the extractive column than for simple distillation columns with high-purity products.

Disturbance Sensitivity

The relative gain array is independent of disturbances. However, an important issue when analyzing processes for feedback control properties is sensitivity to disturbances. The main reason for applying feedback control in distillation is rejection of disturbances that enter the process. In the literature it has been customary to consider the open-loop disturbance gains at steady state when evaluating sensitivity to disturbances. However, for disturbances one should also put emphasis on the high-frequency behavior. In addition, the "direction" of the disturbance effect should be considered in the multivariable case. Some disturbances may be easier to reject than others due to a good alignment with the strong input directions of the plant. Stanley et al. (1985) introduced the relative disturbance gain (RDG) which takes the directions into account. For a particular disturbance z_k the RDG, β_{ik}, is defined for each loop i as the ratio of the change in u_i needed for perfect disturbance rejection in all the outputs to the change in u_i needed for perfect disturbance rejection in the corresponding output y_i when all other inputs are kept constant:

$$\beta_{ik} = \frac{(\partial u_i/\partial z_k)_{yI}}{(\partial u_i/\partial z_k)_{yi,u_{l\neq i}}} \tag{13}$$

Hovd and Skogestad (1991) suggested a measure, the closed-loop disturbance gain (CLDG), δ_{ik}, based on the RDG, but which also takes the disturbance gain g_{dik} into account:

$$\delta_{ik} = \beta_{ik} g_{dik} \tag{14}$$

A matrix of CLDG's may be computed from

$$\Delta = \{\delta_{ik}\} = G_{\text{diag}} G^{-1} G_d \tag{15}$$

where G_{diag} are the diagonal elements of G. Hovd and Skogestad (1991) found that this measure enters nicely into the relation between control offset and disturbances, while the RGA enters in a similar way into the relation between offset and setpoint changes:

$$e_i \approx -\frac{g_{ii}}{g_{ji}} \lambda_{ji} \frac{1}{g_{ii} c_i} r_j + \delta_{ik} \frac{1}{g_{ii} c_i} z_k; \quad \omega < \omega_B \tag{16}$$

This equation provides a good approximation within the band-

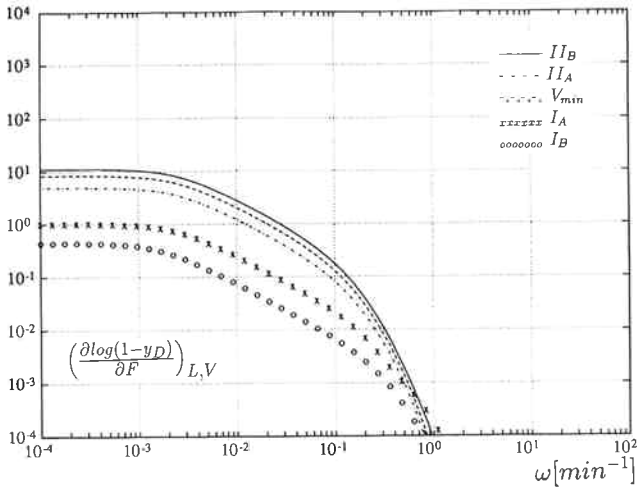

Figure 8. Open-loop disturbance gain for effect of disturbance in *F* on top composition using the LV configuration at different operating points.

width of the closed-loop system when all variables are scaled to be of magnitude one.

In this work we will use the closed-loop disturbance gain as a function of frequency to measure sensitivity to disturbances for the different configurations and operating points. We consider disturbances in the feed rate F, its composition z_F, the entrainer feed rate E, and its composition z_{E1} and z_{E2}. All disturbances are scaled with respect to the maximum expected disturbance size. We expect up to 30% change in the feed rate F, and entrainer feed rate E up to 10 mol % in the azeotropic feed composition z_F and up to 0.10 mol % in the entrainer impurities z_{E1} and z_{E2}.

We find that for the *AHT* column studied here the worst-case disturbances are disturbances in the feeds F and E. Due to limited space we will only present results for these disturbances here. We obtained similar results for all the encountered disturbances. All disturbances are taken into account in the controller design that follows later.

Figure 6 shows the closed-loop disturbance gains for disturbances in F and E as a function of frequency for the LV configuration. Figure 7 shows the same measures for the $(L/D)(V/B)$ configuration. As for the RGA we see that there is a significant difference between the different operating points at low frequencies, while the responses are more similar at higher frequencies. There is, however, still a difference in the interesting frequency region (approximately 0.01 to 1 min^{-1}). The bottom composition r_{12} is most sensitive both to disturbances in E and F. The operating point V_{min} seems to be the best operating point with regards to disturbance sensitivity both at low and high frequencies.

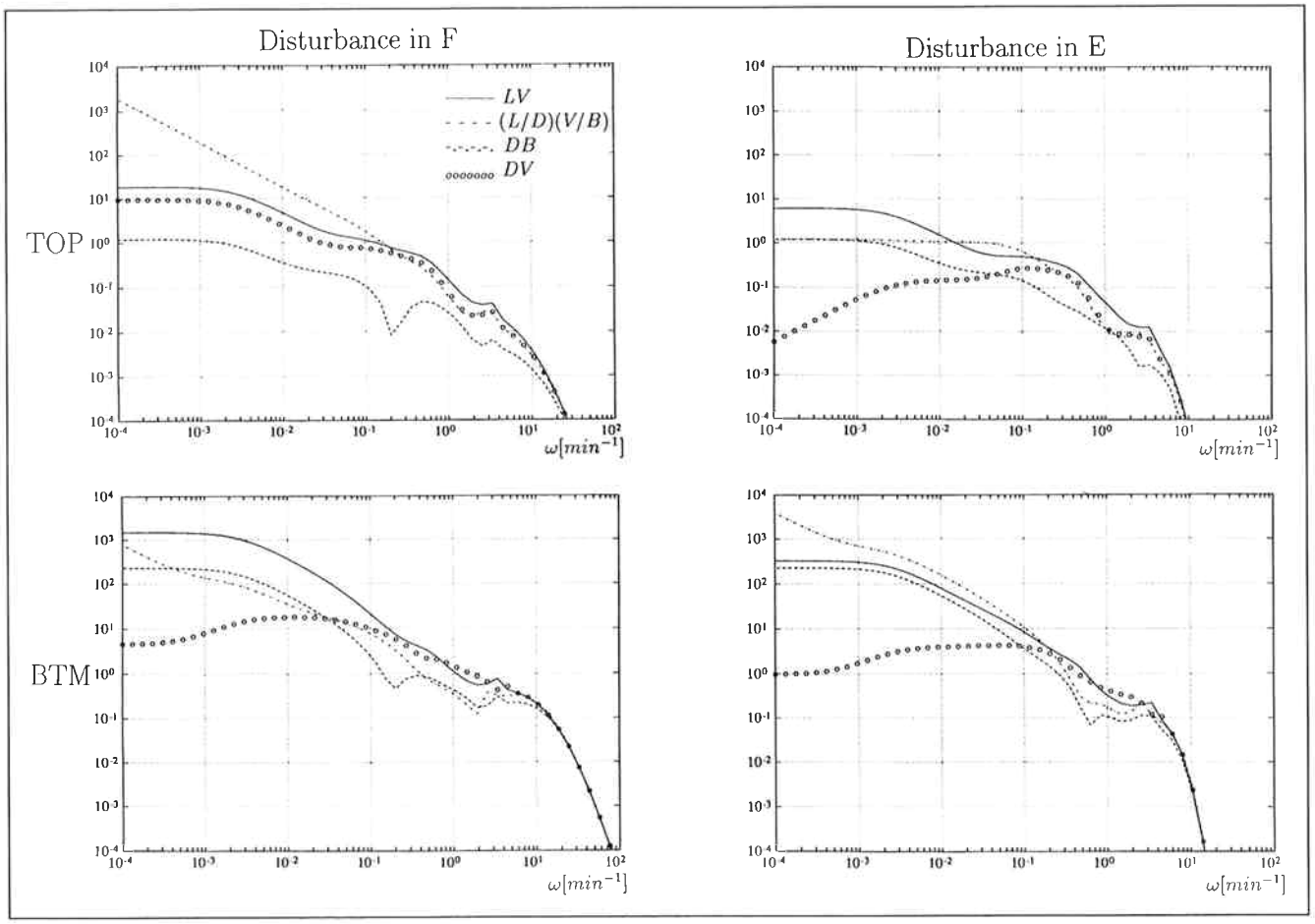

Figure 9. Closed-loop disturbance gains for disturbances in *F* and *E* using configurations LV, DV, DB and (L/D)(V/B) at operating point II_A.

Table 3. Optimal μ Values at Each Operating Point for Acetone-Heptane-Toluene Column

	I_B	I_A	V_{min}	II_A	II_B
LV	1.25	1.20	1.16	1.19	1.47
DV	1.35	1.49	1.53	1.67	1.63
(L/D)(V/B)	1.01	1.03	0.98	0.97	1.12
DB	1.48	1.43	1.35	1.33	1.28

For comparison, consider the open-loop disturbance gain between feed flow F and top composition y_D for the LV configuration in Figure 8. We see that the open-loop disturbance sensitivity gets worse as we get close to region II. From an open-loop analysis one would therefore incorrectly conclude that it is easier to operate as entrainer consumption is increased.

To compare the configurations, consider Figure 9 that shows the CLDG for disturbances in F and E at operating point II_A using the four configurations. We observe a significant difference between the configurations, and the (L/D)(V/B) and DV configurations seem to have the best disturbance rejection properties.

We conclude from the CLDG analysis that there is some difference between the operating points with regards to disturbance sensitivity, but the difference is smaller at higher frequencies than at steady state. The operating point V_{min} (between region I and II) seems to be the best with respect to disturbance rejection.

From the disturbance gains we see that overloading the column with entrainer does not make the control problem easier. This will be true regardless of what bandwidth the controller has; overall the operating point V_{min} will have the best disturbance rejection properties at all frequencies.

Controller Design

The analysis presented above gives an idea of what kind of control performance we may expect at the different operating points using different configurations. However, the ultimate test of achievable performance is, of course, the design of optimal controllers for a chosen objective. In this work we use the structured singular value μ (see, for example, Morari and Zafiriou, 1989) as a design objective. That is, we design for robust performance. The controllers are optimized for setpoint changes as well as disturbances. We limit the structure of the controller to be two single-loop PI controllers. This is done to simplify the computations and because it is the preferred configuration in industry. Single-loop PI controllers have been designed successfully for simple distillation columns (Skogestad et al., 1990a) and seem to be close to optimal (Skogestad and Lundström, 1990).

The uncertainty weight we use on each input in this work is given by:

$$w_I(s) = 0.2\,\frac{5s+1}{0.5s+1} \tag{17}$$

This includes a one-minute deadtime and 20% uncertainty in each input and is the same uncertainty description as used by Skogestad et al. (1990a) for simple distillation columns.

The performance weight was adjusted to give robust performance for at least one operating point:

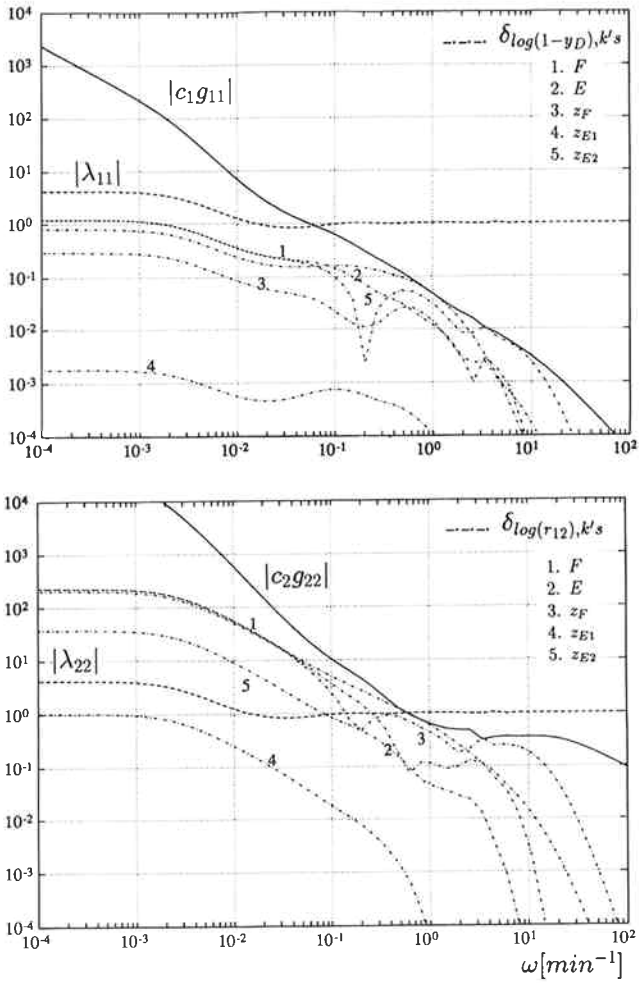

Figure 10. Closed-loop gains, RGA, and CLDG's for all disturbances in the two single loops using the (L/D)(V/B) configuration at operating point II_A.

Controller parameters are given in Table 4.

$$w_P(s) = 0.45\,\frac{15s+1}{15s} \tag{18}$$

This corresponds to a maximum closed-loop time constant of about 30 min for setpoint changes and a maximum amplification of 2.2 of high-frequency disturbances. This performance weight corresponds to somewhat less tight control than what Skogestad et al. (1990a) obtained for simple distillation columns (closed-loop time constant: 20 min). They did, however, optimize only with respect to setpoint changes.

The disturbances were scaled as in the analysis. The outputs are naturally scaled by the logarithm: that is, a magnitude of 1 corresponds to a change in y_D of 0.002 and a change in r_{12} of 0.005.

The results of the optimization in terms of μ values for robust performance are given in Table 3. A μ value less than one implies that the performance criteria are fulfilled for any model uncertainty within the uncertainty weight that was used. The results show that we can only guarantee robust performance (for the weights used) with the (L/D)(V/B) configuration at

Table 4. PI Settings for AHT Column with (L/D) (V/B) Configuration at Operating Point II_A; $C(s) = k\,(1+\tau_I s)/\tau_I s$. Parameters are for scaled compositions (Eqs. 5 and 6).

k_y	k_{r12}	τ_{Iy}	τ_{Ir12}
0.152	1.243	4.101	10.273

Table 5. Optimal μ Values at Each Operating Point for Ethanol-Water-Ethylene Glycol Column

	I_A	V_{min}	II_A	II_B
LV	1.18	1.13	1.14	1.50
DV	1.38	1.40	1.52	1.69
(L/D)(V/B)	1.11	0.99	0.99	0.99
DB	1.52	1.42	1.37	1.14

the operating points V_{min} and II_A. This may be explained by the good disturbance rejection capabilities and low RGA values observed close to the closed-loop bandwidth for this configuration at the two operating points. The (L/D)(V/B) configuration does, however, get close to a μ value of one at the operating points I_A and I_B as well, while II_B seems to be the worst operating point for this configuration. The LV configuration also seems to work best at II_A and V_{min}, but the lowest μ value is 1.16. For the DV configuration there is a clear trend that the control gets worse as we use less entrainer. It seems to be opposite for the DB configuration: that is, control gets easier as we approach region II. These results demonstrate once again how important it is to choose a "good" control configuration. Different configurations will give different conclusions with respect to operability at the different operating points.

In Figure 10 we have plotted the nominal closed-loop gains $|g_{ii}c_i|$ in both loops, together with the RGA and all closed-loop disturbance gains for the (L/D)(V/B) configuration at operating point II_A. The controller is μ-optimal and was designed above with the control parameters given in Table 4.

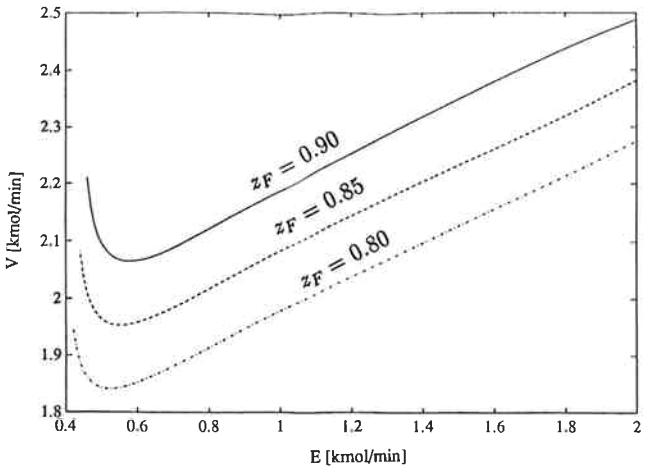

Figure 11. Set of solutions for the AHT column for different azeotropic feed compositions.
Region III is not shown.

From the figure we see that in both loops the closed-loop gain stays above both the RGA and the CLDG's up to the bandwidth. This is necessary to achieve the performance specification (see Eq. 16).

From Figure 10 we note that control of the bottom composition is most difficult. This is expected from the closed-loop disturbance gain analysis which showed that the bottom composition was most sensitive to disturbances. The bandwidth in this loop is much higher than that in the top composition loop which is far less sensitive to disturbances. The difference in bandwidth between the two loops is also advantageous from an interaction point of view. [Because each loop has its main effect in a different frequency region, we avoid possible interaction problems because of nonperfect control (Balchen, 1988).] The distance between the closed-loop gain and the RGA and CLDG's gives the offset e_i according to Eq. 16.

For comparison we optimized controllers also for the ethanol-water-ethylene glycol (EWE) column. Data for the column are given in Table 2. We used the same uncertainty weight as for the AHT column, but the performance requirements were somewhat looser:

$$w_P(s) = 0.40\,\frac{20s+1}{20s} \tag{19}$$

Results of the optimization for the EWE column are given in Table 5. The results are very similar to those for the AHT column, and robust performance can be guaranteed only at operating points V_{min}, II_A and II_B with the (L/D)(V/B) configuration.

Use of Entrainer Feed for Control

So far we have not considered the entrainer as a third degree of freedom in control. The main reason for this is that we did not want to complicate matters too much compared to simple distillation. We did not seem to need this extra degree of freedom. However, there are two reasons why one may want to use the entrainer actively for control. First of all, it may be needed to ensure optimal operation under varying operating conditions. Second, we must avoid that the entrainer feed goes below the minimum needed for the desired separation. The entrainer may be used in a feedback or feedforward manner to accomplish this.

To get an idea when we need to change the entrainer feed to stay at the optimal operating point we need to know how different disturbances affect the optimality curve in Figure 2. It is obvious that the entrainer rate should simply be scaled by a factor $(E/F)^*$, where * denotes the nominal value, for disturbances in F. This may be done in a feedforward manner. As the dynamics for changes in E and F are very similar, dynamic compensation should not be necessary in the feedforward loop.

It is, however, not clear what happens to the trade-off curve for disturbances in feed and entrainer composition. As the separation in the recovery column is easy, we do not expect large disturbances in the entrainer composition and therefore not in the trade-off. Figure 11 shows the trade-off curve for different azeotropic feed compositions. We see that the curve moves mostly in a vertical direction: that is, the value of E_{min}

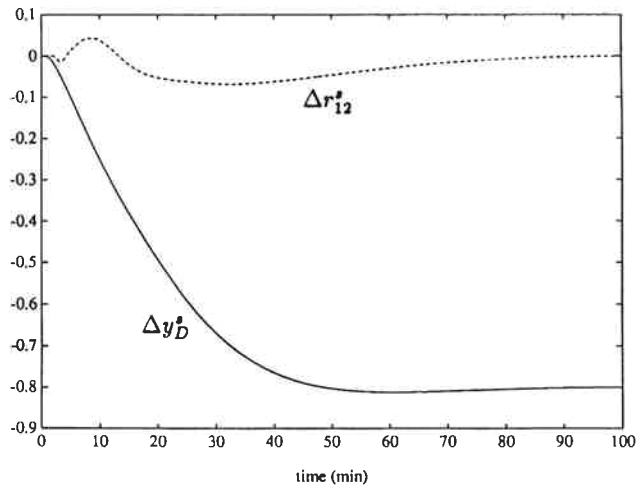

Figure 12. Nonlinear simulation for a set point change in top composition y_D at operating point II_A using the (L/D)(V/B) configuration.

Controller tunings from Table 4. The simulation includes input uncertainties as given in Eq. 17.

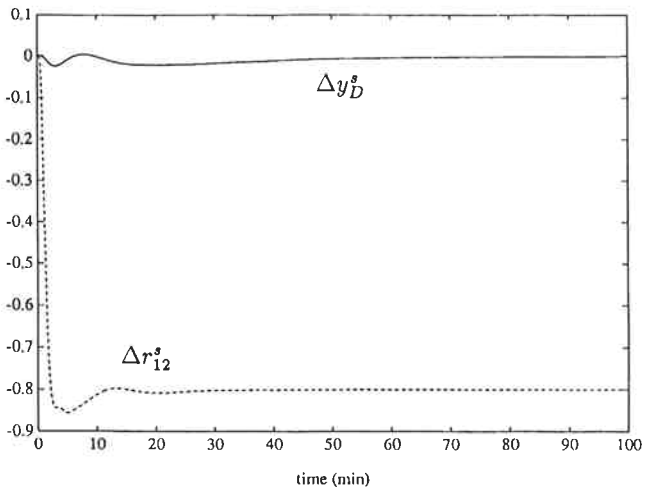

Figure 13. Nonlinear simulation for a set point change in bottom composition r_{12} at operating point II_A using the (L/D)(V/B) configuration.

Controller tunings from Table 4. The simulation includes input uncertainties as given in Eq. 17.

is almost constant, while V_{min} varies. We may, therefore, conclude that to stay close to the optimum and thereby also avoid E_{min} under changing operating conditions, we only have to change the entrainer feed rate for disturbances in the azeotropic feed rate.

We suggest that this may be implemented in a feedforward loop. We do, however, realize that it is impossible to avoid "drift" with feedforward control and that one, therefore, should consider using the entrainer feed in a feedback manner. It is not obvious how this should be done without limiting the flexibility of the column.

Nonlinear Simulations

Figure 12 shows the response to a setpoint change in y_D from 0.998 to 0.9964 ($\Delta y_D^s = -0.8$) in operating point II_A using the (L/D)(V/B) configuration. The controller tunings are the ones obtained from the robust controller design and are given in Table 4. The simulations include a one-minute deadtime and 20% uncertainty in the inputs. Figure 13 shows the response to a setpoint change in the bottom composition r_{12} from 0.005 to 0.001 ($\Delta r_{12}^s = -0.8$) at operating point II_A with the same controller. We see that the bandwidth for the bottom loop is significantly higher than that for the top loop. The simulations demonstrate that setpoint changes are handled easily by the control system and that the interaction between the control loops is small.

Figure 14 shows the response to a 30% increase in azeotropic feed rate F with feedforward action in the entrainer feed rate. The same uncertainty was included in the controller as above, and we also assumed a one-minute deadtime and 20% uncertainty in the entrainer feed rate change: we increased the entrainer feed rate by 24% after one minute. Without the feedforward action, E would fall below E_{min} and the closed-loop system would become unstable. The simulations demonstrate that it is the bottom composition, which is most difficult to control. We do, however, get an acceptable response also for this composition.

On-Line Location of Optimal Operating Point

We discuss here briefly how the optimal operating point may be located on a column that is under operation. We assume that the starting point is in region I, that is, in the nonoptimal region. We know that as we decrease the entrainer feed rate in region I we will simultaneously decrease the boilup until we reach minimum boilup V_{min}, provided both compositions are kept constant (see Figure 2). By decreasing E in a rampwise fashion with both compositions under feedback control, we will observe a decrease in boilup until we pass V_{min}. The ramp change should not be done too fast so that the composition controllers can follow. If the ramp change is done too fast we may go far beyond V_{min} before we actually observe an increase in boilup V. For a sufficiently slow ramp change we may

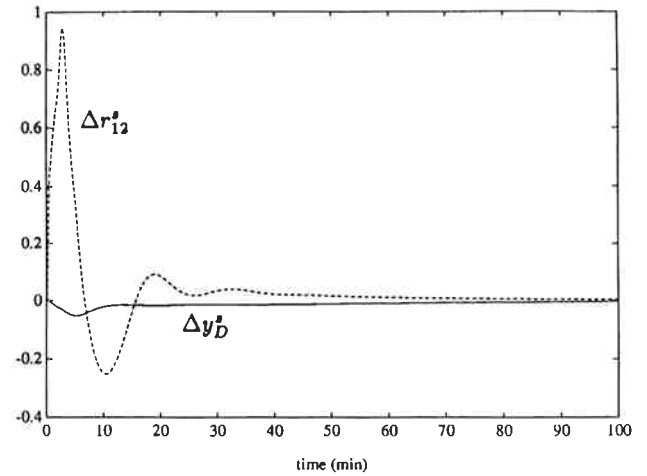

Figure 14. Nonlinear simulation for a 30% increase in azeotropic feed flow rate F at operating point II_A using the (L/D)(V/B) configuration.

Controller tunings from Table 4. Feed forward action for entrainer feed is implemented by keeping (E/F) constant. The simulation includes input uncertainties as given in Eq. 17.

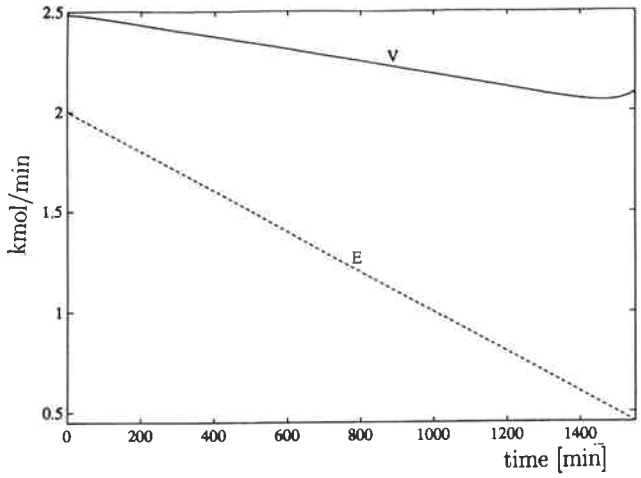

Figure 15. Response in boilup to a ramp decrease in entrainer feed from operating point I_B.

Both compositions under feedback control with the (L/D)(V/B) configuration. Controller tunings from Table 4. The simulation includes uncertainties as given in Eq. 17.

continue the ramp until we observe an increase in boilup. This will provide a fairly accurate location of V_{min}. From this point on one can do small step changes in E until one reaches the desired trade-off between entrainer consumption and boilup.

Figure 15 shows nonlinear simulation results for a ramp decrease in E from operating point I_B using the (L/D)(V/B) configuration. The entrainer feed was decreased at a rate of 0.001 kmol/min. The controller given in Table 4 was used to control compositions. We see that the boilup starts to increase at a value of E around 0.56. The steady-state minimum boilup is at E equal to 0.57. Thus, we are able to determine the point of minimum boilup quite accurately by the proposed method.

Discussion

In this article we studied two columns only, both with heavy entrainers, and one should therefore be careful about making general conclusions. The main results, however, are explained by the fact that the initial responses of the columns are similar at all operating points and also by what is observed in simple distillation. The effects of the nonideal thermodynamics are slow and therefore do not have a strong effect on the high-frequency dynamics which are most important for control. We expect this to be true also for other columns of the same class.

It is clear for the columns studied that it is the bottom product composition that is most sensitive to disturbances and is limiting control performance. However, the ratio r_{12} is also sensitive to the inputs (for example, L and V), which implies that it may be kept above specification at a small expense in terms of boilup and reflux. For instance, one could decrease the ratio r_{12} from 0.005 to 0.001 at operating point II_A of the AHT column by increasing the boilup by only 2.5%. This is not a result of column overdesign as one might expect, as a decrease in number of trays would be expensive in terms of increased boilup. If crucial, we would recommend that the specification for the bottom product is set low enough to never complicate the separation in the recovery column. Another solution may be to add some trays in the stripping section, as this would reduce the high-frequency disturbance sensitivity of the bottom product.

All the presented results indicate that the control problem in the optimal region II is not more difficult than that in region I. These results, however, are based on reasonably tight control. Tight control depends on the choice of a "good" configuration and on obtaining measurements without long delays. The results indicate that the ratio configuration (L/D)(V/B) is the best choice. This is similar to what is found in simple distillation (Skogestad et al., 1990a). The measurement problem has not been treated here and may be a more difficult problem in azeotropic distillation than in simple distillation. As pointed out by several authors (for example, Gilles et al., 1980), it is due to the more difficult temperature profile encountered in these columns. The measurement problem will be studied in a future work.

The existence of a minimum necessary entrainer feed for a given separation may cause problems during the operation. If the azeotropic feed rate is increased by more than 10% at operating point II_A of the AHT column without adjusting the entrainer feed, the column will go closed-loop unstable as the specified separation is infeasible. We propose here using a feedforward loop from azeotropic to entrainer feed to avoid E_{min}. However, this solution is sensitive to uncertainties in flow measurements. A better solution may be to use the entrainer in a feedback scheme in addition to feedforward action. The problem will be to select a measurement that will not limit the flexibility of the column. The control problem will also become more complicated because we get a 3×3 control system.

The problem associated with the minimum entrainer feed may also be reduced by selecting a suboptimal operating point. For the AHT column the operating point V_{min} is not far from the economic optimum but may tolerate significantly larger disturbances in F without the entrainer dropping below E_{min}. This operating point does also have good control properties as seen from the analysis and control design.

Another potential problem, not discussed here, is region III where we have severe right-half plane zeros. If this region is entered dynamically during operation one can experience stability problems. The probability of entering this region is hard to predict analytically because it is a high-order, nonlinear, dynamic problem. One would have to use some kind of Lyapunov function to determine the regions of attraction. Because of the high order and complexity this is too difficult a problem to be handled in this article. In all our simulations, however, we have not been able to perturb the column into a region where we encountered problems resulting from changes in the sign of the gains. Thus, our experience indicates that region III should not pose any problems to practical operation in region II.

The article has not discussed the control of the entrainer recovery column and the coupling between the two columns. The separation in the recovery column will usually be similar to simple distillation. The coupling between the two columns should not be a difficult problem either. A tank for the entrainer feed will be necessary due to variations in the entrainer feed rate, and this will dampen the effect of changes in entrainer flow and composition from the recovery column.

The use of a heavy entrainer discussed here is most widespread in industry today. It is clear, however, that other entrainers may be more favorable both from a steady-state point

of view (Laroche and Morari, 1992) and from a control point of view. One kind of entrainer that may be advantageous is an intermediate boiler. In this case, we have two possible sequences of separation: 1) light component and entrainer in the top of the extractive column; and 2) heavy component and entrainer in the bottom of the extractive column. In both of these cases, the impurities from the extractive column will enter the entrainer product in the recovery column. This entrainer product will be fed back to the bottom of the extractive column in case 1 and to the top in case 2. This implies that the impurities in both cases are fed back to a section where they are easy to separate. Therefore, the entrainer impurities should be easy to handle in the extractive column, and relatively high impurities may be optimal. By the same argument, disturbances in the entrainer impurities should be easy to reject with feedback control, and the performance specification on the ratio (e.g., r_{12}) may be loosened, thereby making control easier.

Conclusions

The control properties both at the optimal operating point (low entrainer feed) and at suboptimal operating points for two extractive columns with heavy entrainer were studied. The analysis of the dynamic model does not indicate a more difficult control problem at the optimal operating point than at other operating points. The robust controller design supports the results of the preliminary analysis. In the optimal region of operation, we obtain controller performance that is comparable to what is achieved for simple distillation columns. The results depend strongly on the choice of a "good" control configuration, and for the columns studied we find the ratio configuration (L/D)(V/B) to be the best choice. The results do depend on relatively tight control as the low-frequency characteristics indicate a more difficult control problem if the bandwidth is significantly lower than what is used in this work. The results are explained by the fact that the initial response in an extractive distillation column is similar to what is found in simple distillation. The effect of nonideal thermodynamics is slow. Therefore, we expect the results obtained to be valid for most extractive columns of the type studied in this work.

The existence of a minimum entrainer feed rate for a desired separation may pose problems in the operation of extractive columns. In this work we proposed a feedforward scheme to avoid $E_{\min}$. This, however, may not be satisfactory, and one should therefore consider using the entrainer in a feedback scheme.

Acknowledgment

Acknowledgment is made to the donors of the Petroleum Research Fund, administered by the American Chemical Society, The Royal Norwegian Council for Scientific and Industrial Research (NTNF), and the Danish Research Council for partial support of this research.

Notation

B = bottom flow, kmol/min
c_i = controller transfer function, loop i
G = process transfer matrix
g_i = process transfer function, loop i
G_d = disturbance gain matrix
g_{dik} = disturbance gain from disturbance k to output i
D = distillate flow, kmol/min
E = entrainer feed flow, kmol/min
e_i = control offset in loop i
F = azeotropic feed flow, kmol/min
L = reflux flow, kmol/min
M_i = liquid holdup on tray i
N = number of theoretical trays
NE = feedtray location for entrainer feed
NF = feedtray location for azeotropic feed
P = pressure
r_{12} = ratio of light to intermediate component in bottom product
r_j = set point change in output j
V = boilup, kmol/min
V_T = condensation rate, kmol/min
w_P = performance weight
w_I = uncertainty weight
y_D = fraction of light component in distillate
z_F = fraction of light component in azeotropic feed
z_{E1} = fraction of light component in entrainer feed
z_{E2} = fraction of intermediate component in entrainer feed
z_k = disturbance k

Greek letters

β_{ik} = relative disturbance gain form disturbance k to output i
δ_{ik} = closed-loop disturbance gain from disturbance k to output i
γ^* = minimized condition number
λ_{ij} = ijth element of the relative gain array
$\mu(mu)$ = structured singular value
τ_L = hydraulic time constant for each tray, min
ω_B = closed-loop bandwidth, min^{-1}

Literature Cited

Abu-Eishah, S. I., and W. L. Luyben, "Design and Control of a Two-Column Azeotropic Distillation System," *Ind. Eng. Chem. Res. Dev.*, **24**, 132 (1985).

Andersen, H. W., L. Laroche, and M. Morari, "Effect of Design on the Control of Homogeneous Azeotropic Distillation Columns," AIChE Meeting, San Francisco (Nov., 1989).

Andersen, H. W., L. Laroche, and M. Morari, "Dynamics of Homogeneous Azeotropic Distillation Columns," *Ind. Eng. Chem. Res.*, **30**, 1846 (1991).

Anderson, J. E., "Multivariable Control of an Azeotropic Distillation Column," *Adv. Instr.*, **42**(2), 469 (1986).

Balchen, J. G., *Process Control: Structures and Applications*, Van Nostrand Reinhold, New York (1988).

Bozenhardt, H. F., "Modern Control Tricks to Solve an Old Problem: Azeotropic Distillation," *Hydroc. Process*, **67**(6), 47 (1988).

Bristol, E. H., "On a New Measure of Interactions for Multivariable Process Control," *IEEE Trans. Automat. Control*, **AC-11**, 133 (1966).

Bristol, E. H., "Recent Results on Interactions in Multivariable Process Control," AIChE Meeting, Chicago (1978).

Doherty, M. F., and G. A. Calderola, "Design and Synthesis of Homogeneous Azeotropic Distillation. 3. The Sequencing of Columns for Azeotropic and Extractive Distillation," *Ind. Eng. Chem. Fund.*, **24**, 474 (1985).

Doyle, J. C., "Structured Uncertainty in Control System Design," *Proc. IEEE Conf. on Decision and Control*, Ft. Lauderdale (1985).

Gilles, E. D., B. Retzbach, and F. Silberberger, "Modelling, Simulation and Control of an Extractive Distillation Column," *ACS Symp. Ser.*, No. 124, Amer. Chem. Soc. (1980).

Hovd, M., and S. Skogestad, "Use of Frequency-Dependent RGA for Control System Analysis, Structure Selection and Design," *Automatica*, in press (1991).

Knapp, J. P., and M. F. Doherty, "Thermal Integration of Homogeneous Azeotropic Distillation Sequences," *AIChE J.*, **36**(7), 969 (1990).

Knight, J. R., and M. F. Doherty, "Optimal Design and Synthesis of Homogeneous Azeotropic Distillation Sequences," *Ind. Eng. Chem. Res*, **28**, 564 (1989).

Laroche, L., and M. Morari, "Entrainer Selection for Homogeneous Azeotropic Distillation," *AIChE J.*, in press (1992).
Levy, S. G., and M. F. Doherty, "Design and Synthesis of Homogeneous Azeotropic Distillation: 4. Minimum Reflux Calculations for Multiple Feed Columns," *Ind. Eng. Chem. Fund.*, **25**, 269 (1985a).
Levy, S. G., and M. F. Doherty, "Design and Synthesis of Homogeneous Azeotropic Distillation. 5. Columns with nonnegligible Heat Effects," *Ind. Eng. Chem. Fund.*, **25**, 279 (1985b).
Morari, M., and E. Zafiriou, *Robust Process Control*, Prentice-Hall, NJ (1989).
Rademaker, O., J. E. Rijnsdorp, and A. Maarleveld, *Dynamics and Control of Continuous Distillation Units*, Elsevier, Amsterdam (1975).
Shinskey, F. G., *Distillation Control*, 1st & 2nd ed., McGraw-Hill, New York (1977, 1984).
Skogestad, S., and M. Morari, "Implication of Large RGA-elements on Control Performance," *Ind. Eng. Chem. Res.*, **26**(11), 2323 (1987a).
Skogestad, S., and M. Morari, "The Effect of Disturbance Directions on Closed-Loop Performance," *Ind. Eng. Chem. Res.*, **26**(10), 2029 (1987b).
Skogestad, S., M. Morari, and J. C. Doyle, "Robust Control of Ill-Conditioned Plants: High-Purity Distillation," *IEEE Trans. Autom. Control*, **33**(12), 1092 (1988).
Skogestad, S., and M. Morari, "Understanding the Dynamic Behavior of Distillation Columns," *Ind. Eng. Chem. Res.*, **27**(10), 1848 (1988).
Skogestad, S., P. Lundström, and E. W. Jacobsen, "Selecting the Best Distillation Control Configuration," *AIChE J.*, **36**(5), 753 (1990a).
Skogestad, S., E. W. Jacobsen, and M. Morari, "Inadequacy of Steady-State Analysis for Feedback Control: Distillate-Bottom Control of Distillation Columns," *Ind. Eng. Chem. Res.*, **29**, 2339 (1990b).
Skogestad, S., and P. Lundström, "Mu-optimal LV-Control of Distillation Columns," *Comp. and Chem. Eng.*, **14**(4/5), 401 (1990).
Stanley, G., M. Marino-Galarraga, and T. J. McAvoy, "Shortcut Operability Analysis: 1. The Relative Disturbance Gain," *Ind. Eng. Chem. Process Des. Dev.*, **24**(4), 1181 (1985).
Witcher, M., and T. J. McAvoy, "Interacting Control Systems: Steady State and Dynamic Measurement of Interaction," *ISA Trans.*, **16**, 35 (1977).
Weigand, W. A., A. K. Jhawar, and T. J. Williams, "Calculation Methods for the Response Time to Step Inputs for Approximate Dynamic Models of Distillation Columns," *AIChE J.*, **18**(6), 1243 (1972).

Manuscript received Jan. 29, 1991 , and revision received Sept. 4, 1991.